

Bandgap Engineering of Monodispersed $\text{Cu}_{2-x}\text{S}_y\text{Se}_{1-y}$ Nanocrystals through Chalcogen Ratio and Crystal Structure

Jian-Jun Wang, Ding-Jiang Xue, Yu-Guo Guo, Jin-Song Hu, and Li-Jun Wan*

Key Laboratory of Molecular Nanostructure and Nanotechnology, Institute of Chemistry, Chinese Academy of Sciences, and Beijing National Laboratory for Molecular Sciences, Beijing 100190, China

S Supporting Information

ABSTRACT: Bandgap engineering is important in light-absorption optimization of nanocrystals (NCs) for applications such as highly efficient solar cells. Herein, a facile one-pot method is developed to synthesize monodispersed ternary alloyed copper sulfide selenide ($\text{Cu}_{2-x}\text{S}_y\text{Se}_{1-y}$) NCs with tunable composition, structure, and morphology. The energy bandgaps can be tuned with the chalcogen ratio, and the crystal structure of the NCs is found to produce an effect on their bandgap and light absorption. The results are significant in bandgap engineering of semiconductor NCs.

Cu-based chalcogenides, as low-cost and eco-friendly materials with the capability of bandgap engineering for highly efficient solar cells, have received considerable attention recently.^{1–13} Progress in the synthetic strategy has demonstrated exciting properties and possible applications of Cu-based chalcogenide colloidal nanocrystals (NCs).^{8–16} These NCs show the advantages of low cost, low-temperature preparation, and economical and convenient post-processing such as spin-casting, dip-coating, and printing, as well as high device performance from quantum confinement effect.^{12,17–27} For example, Cu_{2-x}E (E = S, Se) NCs are extensively studied and have applications in photodetectors, solar cells, nanoscale electric switches, cold cathodes, biosensors, and photothermal therapy.^{13–15,28–32} Their energy gaps match the ideal bandgap range of 1.1–1.7 eV for application as light absorbers.^{12,33–37} Moreover, they could be used as templates to prepare multielement metal chalcogenides such as CuInS_2 , CuInSe_2 , $\text{Cu}_2\text{ZnSnS}_4$, and $\text{Cu}_2\text{ZnSnSe}_4$, which are promising candidates for solar energy conversion.^{5,8,10,18,22,38,39} Monodispersed Cu_2S NCs have been synthesized through several methods and could self-assemble into highly ordered multilayer superlattices with the ability to tune the light absorption.^{21,35,36} By controlling the reactivity of the Se source, Cu_2Se NCs have been prepared, and their potential as photodetectors has been revealed.^{15,33}

Compared to binary materials, ternary alloyed semiconductor nanomaterials are able to produce new properties and inherit the properties from their parent binary materials,^{17,40} and, more importantly, they provide an effective way to control energy bandgap in addition to the size-dependent quantum confinement effects. The energy bandgap can be tuned by controlling the composition of alloyed nanomaterials without changing their size, which is important for materials with a small Bohr radius.¹⁷ Ternary alloyed copper sulfide selenide ($\text{Cu}_{2-x}\text{S}_y\text{Se}_{1-y}$) NCs provide an effective way to finely tune the energy bandgap by

controlling the ratio of chalcogen. Moreover, $\text{Cu}_{2-x}\text{S}_y\text{Se}_{1-y}$ NCs may produce different properties with the inheritance of optoelectronic and biochemical properties from their binary parents, Cu_{2-x}S and Cu_{2-x}Se . However, pure $\text{Cu}_{2-x}\text{S}_y\text{Se}_{1-y}$ NCs have not been extensively studied like their binary parents. To our best knowledge, little work on the synthesis of $\text{Cu}_{2-x}\text{S}_y\text{Se}_{1-y}$ nanomaterials as cubic nanowire bundles has been done to date.⁴¹ This could be due to the difficulty in synthesis of this type of nanomaterials with pure phases. First, copper has two valence states (Cu^+ and Cu^{2+}), which often cause phase separation.^{12,42–44} Second, the parent binary compounds could have different compositions (Cu_2E , CuE_2 , Cu_3E_2 , Cu_5E_4 , Cu_7E_5 , and Cu_{2-x}E ; E = S, Se) and various structures such as monoclinic, cubic, tetragonal, and hexagonal.⁴³ Furthermore, there is no report about Cu_{2-x}S and Cu_{2-x}Se NCs with the same crystallographic structure. Cu_{2-x}S NCs commonly have a monoclinic or hexagonal structure,^{37,45–47} while Cu_{2-x}Se NCs prefer a cubic structure. Finally, in order to get homogeneous alloys, the growth rates of the two constituent materials must be comparable, and the growth conditions for one constituent cannot impede the uniform growth of the other. Commonly, the S precursor and the Se source have different reactivities, which makes it hard to produce the desired alloy with homogeneous structure. Herein, we report a facile one-pot method to prepare pure ternary $\text{Cu}_{2-x}\text{S}_y\text{Se}_{1-y}$ alloyed colloid NCs with engineerable energy bandgap and tunable structure and morphology. It was found that the bandgap and absorption of the ternary NCs is related to not only the chalcogen ratio but also the crystallographic structure.

Diphenyl diselenide and dodecanethiol were selected as selenide and sulfur source, respectively, considering their proper reactivity, solubility, and boiling point. In a typical process, CuCl_2 (33.6 mg), a fixed amount of diphenyl diselenide, and 5 mL of dodecanethiol were added in a two-neck flask. The mixture was heated to 225 °C and reacted for 10 min after the solution was degassed. During the degassing process, Cu^{2+} was reduced to Cu^+ by dodecanethiol and formed copper thiolate with the color change of the solution from yellowish green to turbid white. When the solution is heated, Cu_2S might form via homolytic cleavage of the thiol and alkyl groups, and simultaneously react with diphenyl diselenide, resulting in the formation of $\text{Cu}_{2-x}\text{S}_y\text{Se}_{1-y}$ NCs, as indicated by the color change from yellow to dark red and finally black. The as-synthesized NCs were capped with dodecanethiol, which makes them disperse freely in organic solvents including toluene and hexane.

Received: August 25, 2011

Published: October 24, 2011

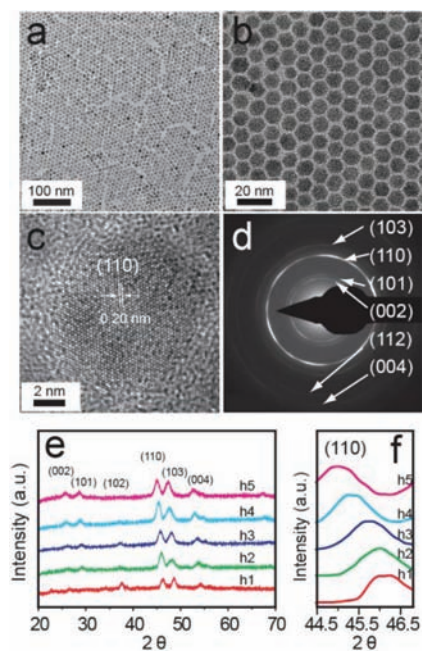


Figure 1. Hexagonal ternary $\text{Cu}_{2-x}\text{S}_x\text{Se}_{1-y}$ NCs. (a,b) Low- and high-magnification TEM images, (c) HRTEM image, and (d) SAED pattern of as-synthesized $\text{Cu}_{2-x}\text{S}_x\text{Se}_{1-y}$ NCs with Cu/S/Se of 62:7:31. (e,f) XRD patterns of samples with various Cu/S/Se ratios: h1, 63:37:0; h2, 63:27:10; h3, 62:19:19; h4, 64:13:23; h5, 62:7:31.

Figure 1a,b shows the typical transmission electron microscopy (TEM) images of the $\text{Cu}_{2-x}\text{S}_x\text{Se}_{1-y}$ NCs synthesized by adding 80 mg of diphenyl diselenide. The low-magnification TEM images indicate that the as-synthesized NCs are nearly monodispersed with an average diameter of 9.4 ± 0.6 nm, and they easily self-assemble into a two-dimensional (2D) array as a result of uniform size.¹⁰ It should be pointed out that the synthesized ternary NCs could self-assembly into a superlattice, which implies the narrow size distribution of NCs (Figure S1, see Supporting Information (SI)).^{21,35} Figure 1c shows a high-resolution (HR) TEM image of an individual NC. The lattice fringes show that the NCs are well crystallized, and the observed d -spacing can be indexed to the (110) plane of hexagonal $\text{Cu}_{2-x}\text{S}_x\text{Se}_{1-y}$. The selected area electron diffraction (SAED) pattern (Figure 1d) shows six rings, which are well consistent with the diffraction patterns from hexagonal crystal structure. The chemical composition of sample was measured by energy-dispersive X-ray spectroscopy (EDS). The measured Cu/S/Se atomic ratios are listed in Table S1 (SI). They confirm that Se content in the as-synthesized NCs increases with the amount of added diphenyl diselenide. In addition, all the samples have a similar Cu content because they have the same Cu source.

The structure of the as-synthesized NCs was further confirmed by X-ray diffraction (XRD). Figure 1e presents XRD patterns of the $\text{Cu}_{2-x}\text{S}_x\text{Se}_{1-y}$ NCs with different compositions. Pattern h1 in Figure 1e was recorded from Cu_{2-x}S NCs, which underwent a phase transition from low-temperature monoclinic crystal structure to high-temperature hexagonal phase at approximately 100 °C.⁴⁸ In view of the relatively high synthesis temperature, the hexagonal structure was thermodynamically favored, and the resulting XRD pattern confirmed that the as-synthesized Cu_{2-x}S NCs retain metastable hexagonal structure (JCPDS card no. 26-1116) at room temperature. The cooling

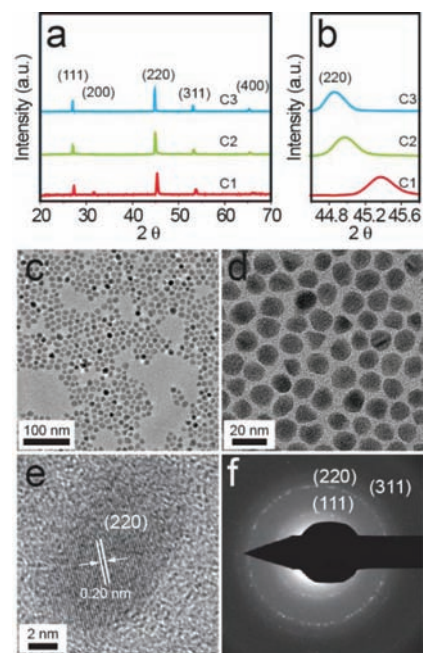


Figure 2. Cubic ternary $\text{Cu}_{2-x}\text{S}_x\text{Se}_{1-y}$ NCs. (a,b) XRD patterns of samples with various Cu/S/Se ratios: c1, 66:20:14; c2, 59:5:36; c3, 52:3:45. (c,d) TEM images, (e) HRTEM image, and (f) SAED pattern of as-synthesized $\text{Cu}_{2-x}\text{S}_x\text{Se}_{1-y}$ NCs with Cu/S/Se of 59:5:36.

process during synthesis did not cause a phase change back to monoclinic phase, which agrees with the previous studies.^{47,49} Patterns h2–h4 were recorded from the ternary alloyed products with various S/Se ratios. The diffraction data suggest that all the samples have a hexagonal structure with slightly different lattice parameters (Table S1 in SI). Figure 1f shows the amplified (110) diffraction peaks of the samples. It can be seen that the peaks successively shift to lower degrees with the increase of Se content in the samples. This shift could be attributed to an increase in the size of the crystallographic unit cell due to the incorporation of more Se which has a larger atomic size than S.⁴¹

Note that the cubic phase is more stable for Cu_{2-x}Se at the relatively high synthesis temperature.^{12,44} In the present experiments, however, pure cubic ternary alloyed NCs could not be prepared, even at high temperatures up to 255 °C. This may be attributed to the difference in source materials, solvent effect, and reaction time.⁵⁰ In order to tune the structure of $\text{Cu}_{2-x}\text{S}_x\text{Se}_{1-y}$ NCs, we have tried different reaction conditions and found that the cubic ternary alloyed NCs could be obtained when oleylamine was used as solvent with a fixed amount of dodecanethiol as S source and keeping the total volume of the solution constant. After the mixture was heated at 255 °C for more than 15 min, $\text{Cu}_{2-x}\text{S}_x\text{Se}_{1-y}$ NCs with pure cubic phase were formed, as confirmed by the XRD patterns shown in Figure 2a, which can be indexed to the bulk cubic Cu_{2-x}S (JCPDS card no. 53-0522) and Cu_{2-x}Se (JCPDS card no. 06-0680) crystals. Furthermore, we observed the diffraction peak shift with the change of S/Se ratio in cubic $\text{Cu}_{2-x}\text{S}_x\text{Se}_{1-y}$ NCs as well, similar to that of hexagonal NCs. Figure 2b shows amplified curves of the (220) diffraction peaks of the samples with the highest intensity. It is clearly seen that the peaks shift to higher degrees with the increase of S/Se ratio.³⁷ The successive shift in the diffraction peaks can be ascribed to the decrease in the unit cell size resulting from the incorporation of more S with a smaller atomic size than Se.

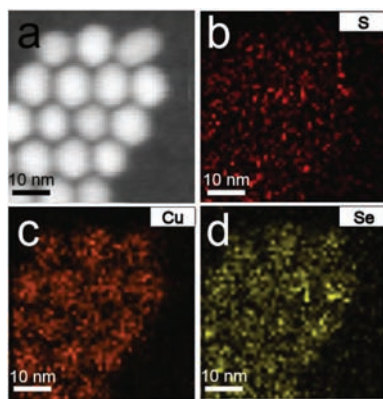


Figure 3. (a) STEM image, (b) S elemental map, (c) Cu elemental map, and (d) Se elemental map of hexagonal $\text{Cu}_{2-x}\text{S}_y\text{Se}_{1-y}$ NCs.

The synthetic conditions and measured Cu/S/Se ratios for cubic ternary NCs are listed in Table S2 (see SI). It shows that the S/Se ratio is proportional to the ratio of the amount of added dodecanethiol and diphenyl diselenide. It should be mentioned that both the hexagonal and the cubic $\text{Cu}_{2-x}\text{S}_y\text{Se}_{1-y}$ NCs showed high environmental stability with no obvious change in the XRD patterns of the samples after storage in air over three months (see Figure S4 in SI).

The representative low-magnification TEM images of the cubic $\text{Cu}_{2-x}\text{S}_y\text{Se}_{1-y}$ NCs with Cu/S/Se of 59:5:36 are shown in Figure 2c,d. It can be seen that the morphology of cubic NCs is slightly different from that of hexagonal NCs, but they also have a very narrow size distribution with an average diameter of 12.8 ± 1.5 nm. The lattice fringes in the HRTEM image of an individual NC (Figure 2e) indicate that the NC is a single crystal with d -spacing indexed to the (220) plane of cubic $\text{Cu}_{2-x}\text{S}_y\text{Se}_{1-y}$. The SAED pattern (Figure 2f) shows three diffraction rings, corresponding to (111), (220), and (311) of cubic crystal, respectively.

In addition, it is found that the size of the as-synthesized NCs is dependent on the amount of added dodecanethiol. For example, the sizes changed from 6.1 ± 0.7 to 7.2 ± 0.8 to 13.1 ± 0.7 nm by tuning the amount of dodecanethiol from 0.1 to 1.0 to 2.5 mL while keeping the Se amount constant (see Figure S5 in SI). Also, the type of copper source affected the shape of NCs to some extent. When CuCl_2 was used as Cu source, the as-synthesized NCs tended to be spherical, while when copper oleate was used as Cu source, NCs with triangle shape appeared, as shown in Figure S6 (see SI). The shape change could be attributed to the difference in reactivity of the Cu source and the capping effect of dodecanethiol on different crystal facets. A detailed investigation is still in progress.

To identify the element distribution of the as-synthesized $\text{Cu}_{2-x}\text{S}_y\text{Se}_{1-y}$ NCs, STEM-EDS elemental maps of $\text{Cu}_{2-x}\text{S}_y\text{Se}_{1-y}$ NCs were recorded. Representative results are shown in Figure 3. The three elements Cu, S, and Se are identified in all the NCs, and no apparent element separation or aggregation is observed, indicating that all three elements are homogeneously distributed within the NCs. X-ray photoelectron spectroscopy (XPS) analysis shows that the binding energy of Cu $2p_{3/2}$ is 932.4 eV (Figure S7 in SI), which corresponds to monovalent copper.^{15,33,51,52} The result indicates that Cu^{2+} is reduced to Cu^+ by dodecanethiol, consistent with the stoichiometry of the NCs.^{35,45,49}

The bandgap of bulk Cu_{2-x}S is dependent on stoichiometry and increases with a decrease in copper content in the crystals.³⁷ For example, the bandgap is 1.2 eV for Cu_2S , 1.5 eV for $\text{Cu}_{1.8}\text{S}$, and 2.0 eV for CuS .^{13,37} In this paper, we found the bandgap

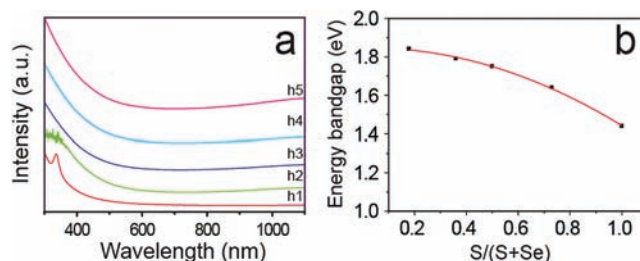


Figure 4. (a) UV-vis absorption spectra of as-synthesized hexagonal $\text{Cu}_{2-x}\text{S}_y\text{Se}_{1-y}$ NCs with various Cu/S/Se ratios: h1, 63:37:0; h2, 63:27:10; h3, 62:19:19; h4, 64:13:23; h5, 62:7:31. (b) Relationship between the bandgaps of the $\text{Cu}_{2-x}\text{S}_y\text{Se}_{1-y}$ NCs and the molar ratio of S/(S + Se).

can also be changed by tuning the chalcogen ratio in ternary $\text{Cu}_{2-x}\text{S}_y\text{Se}_{1-y}$ NCs. UV-vis absorption spectra of hexagonal $\text{Cu}_{2-x}\text{S}_y\text{Se}_{1-y}$ NCs were recorded and used to estimate the bandgap of the $\text{Cu}_{2-x}\text{S}_y\text{Se}_{1-y}$ NCs (Figure 4a). Curve h1 in Figure 4a shows that the Cu_{2-x}S NCs have a strong absorbance from 300 to 600 nm, with an obvious blue-shift absorbing band peak located at ~ 340 nm, which is similar to the previously reported results on Cu_{2-x}S NCs.^{37,42,46,53} The absorbance reaches a minimum at about 850 nm and then rises at longer wavelengths due to free carrier intraband absorption.^{14,33,37} For the ternary $\text{Cu}_{2-x}\text{S}_y\text{Se}_{1-y}$ NCs, the absorption edges shift to lower wavelength as the Se content increases, corresponding to the larger bandgap of bulk Cu_{2-x}Se than bulk Cu_{2-x}S . All spectra have a minimum absorption at about 700–850 nm, but do not show absorbing band peaks around 300–600 nm, except for strong absorbance, consistent with previous reports.⁴¹ Recently, it has been reported that the light absorption of $\text{Cu}_{1.97}\text{S}$ NCs changes upon arrangement into supercrystals.³⁵ The UV-vis spectra were accordingly measured before and after deassembly of the ternary alloyed NCs in toluene. The results are similar to those previously reported for $\text{Cu}_{1.97}\text{S}$ NCs, as shown in Figure S8 in SI.³⁵ The absorption spectra from deassembled NCs were used to estimate the bandgaps of NCs by using the same method based on the relation of $(\alpha h\nu)^{1/2}$ versus $h\nu$ (where α is absorbance, h is Planck's constant, and ν is frequency). The relationship between the bandgaps and the molar ratio of S/(S + Se) (i.e., S content) is shown in Figure 4b. These results imply that the energy bandgap of the ternary alloy can be tuned from 1.44 to 1.85 eV by adjusting the S content, which is largely blue-shifted compared with the binary copper chalcogenides. The large shift here is probably due to the quantum size effect from the as-synthesized NCs, which is in agreement with previous reported binary copper chalcogenide NCs.^{15,33,37,46,53}

More interestingly, it was found that the bandgaps of $\text{Cu}_{2-x}\text{S}_y\text{Se}_{1-y}$ NCs can also be tuned by changing the crystallographic structure of the NCs. For example, the hexagonal $\text{Cu}_{2-x}\text{S}_y\text{Se}_{1-y}$ NC with Cu/S/Se = 64:13:23 has a bandgap of 1.79 eV, but the bandgap of cubic NC with similar Cu/S/Se = 64:10:26 decreases to 1.53 eV, although the S content is slightly lower in the latter, and the average size of NCs decreases from 9.1 ± 0.9 to 7.2 ± 0.8 nm, which usually causes an increase in bandgap as reported in the literature.^{37,41} Additionally, the absorption of cubic $\text{Cu}_{2-x}\text{S}_y\text{Se}_{1-y}$ NCs increases more rapidly at longer wavelengths compared to that of hexagonal NCs, as shown in Figure S9 in SI. The reasons for the difference in absorption between cubic and hexagonal NCs with similar

composition are not very clear yet. Detailed theoretical and experimental investigations are underway.

In summary, monodispersed ternary alloyed $\text{Cu}_{2-x}\text{S}_y\text{Se}_{1-y}$ NCs are prepared through a facile one-pot method. The structure of the synthesized NCs can be controlled from hexagonal to cubic by changing the reaction conditions. The size and morphology of the cubic phase NCs are related to the amount of dodecanethiol and the type of copper source. The compositions of both the hexagonal and the cubic NCs are easily tuned by adjusting the amounts of diphenyl diselenide and dodecanethiol. UV-vis absorption analysis indicates the bandgap of the $\text{Cu}_{2-x}\text{S}_y\text{Se}_{1-y}$ NCs can be tuned by the chalcogen ratio in the ternary alloyed NCs, as well as the crystal structure.

ASSOCIATED CONTENT

S Supporting Information. Analytical data, spectra, and images. This material is available free of charge via the Internet at <http://pubs.acs.org>.

AUTHOR INFORMATION

Corresponding Author

wanlijun@iccas.ac.cn

ACKNOWLEDGMENT

This work is supported by the National Key Project on Basic Research (Grants 2011CB935700, 2011CB808700 and 2009CB930400), the National Natural Science Foundation of China (Grants 21173237 and 20821003), and the Chinese Academy of Sciences.

REFERENCES

- Fan, X.; Meng, X.-M.; Zhang, X.-H.; Shi, W.-S.; Zhang, W.-J.; Zapien, J. A.; Lee, C.-S.; Lee, S.-T. *Angew. Chem., Int. Ed.* **2006**, *45*, 2568.
- Todorov, T.; Reuter, K.; Mitzi, D. *Adv. Mater.* **2010**, *22*, E156.
- Tian, B.; Kempa, T. J.; Lieber, C. M. *Chem. Soc. Rev.* **2008**, *38*, 16.
- Brian, M.; Dunn, G.; Brian, A.; Korgel, A. *J. Am. Chem. Soc.* **2008**, *130*, 16770.
- Guo, Q.; Hillhouse, H.; Agrawal, R. *J. Am. Chem. Soc.* **2009**, *131*, 11672.
- Mitzi, D. B.; Yuan, M.; Kellock, A. J.; Chey, S. J.; Gunawan, O. *Chem. Mater.* **2009**, *22*, 1010.
- Nose, K.; Omata, T.; Otsuka-Yao-Matsuo, S. *J. Phys. Chem. C* **2009**, *113*, 3455.
- Steinhagen, C.; Panthani, M.; Akhavan, V.; Goodfellow, B.; Koo, B.; Korgel, B. *J. Am. Chem. Soc.* **2009**, *131*, 12554.
- Guo, Q.; Ford, G.; Yang, W.; Walker, B.; Stach, E.; Hillhouse, H.; Agrawal, R. *J. Am. Chem. Soc.* **2010**, *132*, 2844.
- Wang, J.-J.; Wang, Y.-Q.; Cao, F.-F.; Guo, Y.-G.; Wan, L.-J. *J. Am. Chem. Soc.* **2010**, *132*, 12218.
- Guo, Q.; Kim, S.; Kar, M.; Shafarman, W.; Birkmire, R.; Stach, E.; Agrawal, R.; Hillhouse, H. *Nano Lett.* **2008**, *8*, 2982.
- Deka, S.; Genovese, A.; Zhang, Y.; Miszta, K.; Bertoni, G.; Krahne, R.; Giannini, C.; Manna, L. *J. Am. Chem. Soc.* **2010**, *132*, 8912.
- Wu, Y.; Wadia, C.; Ma, W.; Sadtler, B.; Alivisatos, A. *Nano Lett.* **2008**, *8*, 2551.
- Li, Y.; Lu, W.; Huang, Q.; Li, C.; Chen, W. *Nanomedicine* **2010**, *5*, 1161.
- Choi, J.; Kang, N.; Yang, H. Y.; Kim, H. J.; Son, S. U. *Chem. Mater.* **2010**, *22*, 3586.
- Rivest, J. B.; Swisher, S. L.; Fong, L.-K.; Zheng, H.; Alivisatos, A. P. *ACS Nano* **2011**, *5*, 3811.
- Regulacio, M.; Han, M. *Acc. Chem. Res.* **2010**, *43*, 621.
- Shavel, A.; Arbiol, J.; Cabot, A. *J. Am. Chem. Soc.* **2010**, *132*, 4514.
- Choi, S.; Kim, E.; Hyeon, T. *J. Am. Chem. Soc.* **2006**, *128*, 2520.
- Pan, D.; An, L.; Sun, Z.; Hou, W.; Yang, Y.; Yang, Z.; Lu, Y. *J. Am. Chem. Soc.* **2008**, *130*, 5620.
- Zhuang, Z.; Peng, Q.; Zhang, B.; Li, Y. *J. Am. Chem. Soc.* **2008**, *130*, 10482.
- Riha, S.; Parkinson, B.; Prieto, A. *J. Am. Chem. Soc.* **2009**, *131*, 12054.
- Smith, A. M.; Nie, S. *Acc. Chem. Res.* **2009**, *43*, 190.
- Park, S.; An, J.; Jung, I.; Piner, R. D.; An, S. J.; Li, X.; Velamakanni, A.; Ruoff, R. S. *Nano Lett.* **2009**, *9*, 1593.
- Peng, X. *Acc. Chem. Res.* **2010**, *43*, 1387.
- Huynh, W. U.; Dittmer, J. J.; Alivisatos, A. P. *Science* **2002**, *295*, 2425.
- Sun, B.; Marx, E.; Greenham, N. C. *Nano Lett.* **2003**, *3*, 961.
- Sakamoto, T.; Sunamura, H.; Kawaura, H.; Hasegawa, T.; Nakayama, T.; Aono, M. *Appl. Phys. Lett.* **2003**, *82*, 3032.
- Hessel, C. M.; Pattani, P. V.; Rasch, M.; Panthani, M. G.; Koo, B.; Tunnell, J. W.; Korgel, B. A. *Nano Lett.* **2011**, *11*, 2560.
- Liu, J.; Xue, D. *J. Mater. Chem.* **2010**, *21*, 223.
- Chen, J.; Deng, S.; Xu, N.; Wang, S.; Wen, X.; Yang, S.; Yang, C.; Wang, J.; Ge, W. *Appl. Phys. Lett.* **2002**, *80*, 3620.
- Dai, H. *Acc. Chem. Res.* **2002**, *35*, 1035.
- Liu, Y.; Dong, Q.; Wei, H.; Ning, Y.; Sun, H.; Tian, W.; Zhang, H.; Yang, B. *J. Phys. Chem. C* **2011**, *115*, 9909.
- Riha, S. C.; Johnson, D. C.; Prieto, A. L. *J. Am. Chem. Soc.* **2011**, *133*, 1383.
- Kriegel, I.; Rodriguez-Fernandez, J.; Como, E. D.; Lutich, A. A.; Szeifert, J. M.; Feldmann, J. *Chem. Mater.* **2011**, *23*, 1830.
- Li, X.; Shen, H.; Niu, J.; Li, S.; Zhang, Y.; Wang, H.; Li, L. S. *J. Am. Chem. Soc.* **2010**, *132*, 12778.
- Zhao, Y.; Pan, H.; Lou, Y.; Qiu, X.; Zhu, J. J.; Burda, C. *J. Am. Chem. Soc.* **2009**, *131*, 4253.
- Xu, J.; Lee, C.-S.; Tang, Y.-B.; Chen, X.; Chen, Z.-H.; Zhang, W.-J.; Lee, S.-T.; Zhang, W.; Yang, Z. *ACS Nano* **2010**, *4*, 1845.
- Katagiri, H.; Jimbo, K.; Maw, W.; Oishi, K.; Yamazaki, M.; Araki, H.; Takeuchi, A. *Thin Solid Films* **2009**, *517*, 2455.
- El-Sayed, M. A. *Acc. Chem. Res.* **2004**, *37*, 326.
- Xu, J.; Tang, Y.-B.; Chen, X.; Luan, C.-Y.; Zhang, W.-F.; Zapien, J. A.; Zhang, W.-J.; Kwong, H.-L.; Meng, X.-M.; Lee, S.-T.; Lee, C.-S. *Adv. Funct. Mater.* **2010**, *20*, 4190.
- Kumar, P.; Gusain, M.; Nagarajan, R. *Inorg. Chem.* **2011**, *50*, 3065.
- Xie, Y.; Zheng, X.; Jiang, X.; Lu, J.; Zhu, L. *Inorg. Chem.* **2002**, *41*, 387.
- Kashida, S.; Shimosaka, W.; Mori, M.; Yoshimura, D. *J. Phys. Chem. Solids* **2003**, *64*, 2357.
- Choi, S. H.; An, K.; Kim, E. G.; Yu, J. H.; Kim, J. H.; Hyeon, T. *Adv. Funct. Mater.* **2009**, *19*, 1645.
- Liu, Z.; Xu, D.; Liang, J.; Shen, J.; Zhang, S.; Qian, Y. *J. Phys. Chem. B* **2005**, *109*, 10699.
- Larsen, T. H.; Sigman, M.; Ghezlbash, A.; Doty, R. C.; Korgel, B. A. *J. Am. Chem. Soc.* **2003**, *125*, 5638.
- Buerger, M.; Wuensch, B. *J. Science* **1963**, *141*, 276.
- Sigman, M. B., Jr.; Ghezlbash, A.; Hanrath, T.; Saunders, A. E.; Lee, F.; Korgel, B. A. *J. Am. Chem. Soc.* **2003**, *125*, 16050.
- Zhang, H.; Zhang, Y.; Yu, J.; Yang, D. *J. Phys. Chem. C* **2008**, *112*, 13390.
- Zhang, W.; Zhang, X.; Zhang, L.; Wu, J.; Hui, Z.; Cheng, Y.; Liu, J.; Xie, Y.; Qian, Y. *Inorg. Chem.* **2000**, *39*, 1838.
- Silvester, E. J.; Grieser, F.; Sexton, B. A.; Healy, T. W. *Langmuir* **1991**, *7*, 2917.
- Wang, Y.; Hu, Y.; Zhang, Q.; Ge, J.; Lu, Z.; Hou, Y.; Yin, Y. *Inorg. Chem.* **2010**, *49*, 6601.